X-ray Crystal Structure, Partitioning Behavior, and Molecular Modeling Study of Piracetam-Type Nootropics: Insights into the Pharmacophore

Cosimo Altomare, Saverio Cellamare, Angelo Carotti,* Giovanni Casini, and Marcello Ferappi

Dipartimento Farmaco-Chimico, University of Bari, I-70125 Bari, Italy

Enrico Gavuzzo and Fernando Mazza

Istituto di Strutturistica Chimica, CNR, I-00016 Monterotondo Stazione, Roma, and Dipartimento di Chimica, University of L'Aquila, I-67010 L'Aquila, Italy

Pierre-Alain Carrupt, Patrick Gaillard, and Bernard Testa

Institut de Chimie Thérapeutique, Ecole de Pharmacie, Université de Lausanne, BEP, CH-1015 Lausanne, Switzerland

Received April 19, 1994®

To detect possible molecular determinants of amnesia-reverting activity, the conformational properties of a number of rigid and flexible piracetam-type cognition enhancers have been assessed by X-ray diffraction, NMR spectroscopy, and *ab initio* and high-temperature-quenched molecular dynamics (QMD) calculations. The structures of the preferred conformers in solution derived from ^{1}H-NMR spectral analysis were in good agreement with those found by QMD calculations. Interestingly, the calculation of the average molecular lipophilicity potential on the water-accessible surface of the selected conformers was helpful in interpreting the partitioning behavior observed by measuring octanol-water partition coefficients and capacity factors in reversed-phase high-performance liquid chromatography. While lipophilicity does not play a relevant role, the distance between polar groups, accounted for by the distance between carbonyl oxygens, emerges as a factor, among others, which should influence the amnesia-reversal activity of piracetam-type nootropics.

Introduction

Cognitive deficits and memory loss are frequently associated with aging (benign senescent forgetfulness), senile dementia, and primary degenerative dementia (Alzheimer's disease).[1] Due to demographic changes and the strong increase in mean life expectancy in developed countries, the incidence of cognitive disorders in the population is likely to grow.[2] The development of therapeutic approaches in the treatment of cognitive disorders is thus a real and urgent problem nowadays, and strategies to provide alleviation of cognitive deficits and/or slow down brain degenerative processes have emerged.[2-5] Among the possible therapeutic interventions, 2-pyrrolidone derivatives[6] such as piracetam and related nootropics are currently used for their facilitatory effects in learning and memory in animal models.

There is evidence that piracetam and piracetam-like nootropics might alter presynaptic cholinergic functions, possibly by enhancing high-affinity neuronal uptake of choline, and elevate muscarinic receptor density in the frontal cortex of aged mice.[7,8] An enhancement of glutaminergic hippocampal and cortical systems and the induction of hippocampal long-term potentiation in rodent brain slices have been also observed.[9-12] Despite these evidences, the mechanism of action of the piracetam-type cognition enhancers is far from being understood. Even though clinical trials have frequently yielded conflicting results,[13] in preclinical studies protective effects of nootropics against various insults to the central nervous system are continuously documented.[14,15]

With the aim to obtain information on structural requisites which might lead to a more rational design of new potentially useful nootropic agents, several recent studies examined the structural and conformational properties of pyrrolidone-containing amnesia-reverting compounds[16-18] and proposed possible pharmacophoric models.[19]

Some years ago, some of us reported the synthesis and cognition-activating properties of some mono- and bicyclic lactam derivatives (Chart 1).[20] Here we report the results of a detailed study of their three-dimensional structures obtained from X-ray crystallography, NMR spectroscopy, and molecular modeling. The limited conformational mobility of most examined compounds is expected to yield more accurate detection of possible molecular determinants of amnesia-reverting activity, our final goal being the obtention of insights helpful for the design of further nootropic drugs. The partitioning behavior of these lactam compounds was also investigated; polar and apolar interactions encoded in the lipophilicity parameters were examined in order to identify structural properties possibly involved in modulating the *in vivo* activity of nootropics.

Results and Discussion

Crystal Structure Description. The atomic numbering adopted for compounds **2** and **4** together with the valence bond lengths and angles for their non-H atoms are reported in Figure 1, whereas crystal data for the same compounds are reported in Table 1.

The geometries of the two *cis* amide groups of compound **2** are comparable within experimental errors. The lengthening of the C(1)-N(2) and N(5)-C(6) bonds (1.358(4) and 1.351(4) Å, respectively) are associated

* To whom correspondence should be addressed.

® Abstract published in *Advance ACS Abstracts*, December 1, 1994.

0022-2623/95/1838-0170$09.00/0

Chart 1

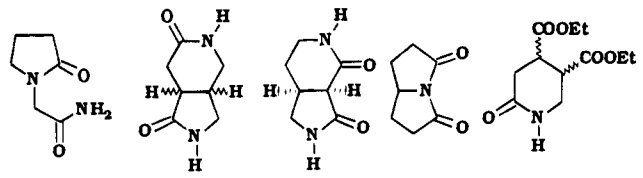

1, Piracetam 2 (cis) 3 (trans) 4 5 6 (cis) 7 (trans)

with C(1)–O(1) and C(6)–O(6) bond lengths of 1.244(4) and 1.239(4) Å.

As for the two *cis* amide groups of compound **4**, we noted that small but significant differences characterize their geometries. While the N(2)–C(3) and C(3)–O(3) bond lengths are 1.341(3) and 1.226(3) Å, respective values of 1.330(3) and 1.242(2) Å have been found for the N(5)–C(4) and C(4)–O(4) bond lengths.

The relevant torsion angles computed according to the convention of Klyne and Prelog[21] for **2** and **4** are reported in Table 2, while perspective views of the two compounds, **2** and **4**, are shown in Figure 2.

The six-membered ring of **2** assumes a boat conformation characterized by two pseudomirror planes, one passing through atoms C(4) and C(7), the other bisecting the amide bond N(5)–C(6) and the ring-junction bond C(8)–C(9). The five-membered ring of **2** presents low puckering since the sum of the absolute values of the internal torsion angles is only 19.3(1)°; it assumes a flat half-chair conformation characterized by a pseudo-2-fold axis-bisecting atom, C(1). The fusion between the two rings of **2** is of the *cis*-type as seen from the torsion angles of junction, 5.6(3)° and 4.7(3)° for the six- and five-membered ring, respectively, and both of the same sign. The H(8) and H(9) atoms of the ring junction are both equatorial with respect to the six-membered ring and are practically eclipsed; the torsion angle H(8)–C(8)–C(9)–H(9) is only 0(2)°, and the contact H(8)···H(9) is reduced to 2.31(3) Å, a value compared to the sum of their van der Waals radii. The folding between the two rings of **2** can be described by the angle between the mean planes through the two rings' non-H atoms which is 99.5(1)°.

The six-membered ring of **4** assumes a half-chair conformation characterized by a pseudo-2-fold axis bisecting the C(4)–N(5) and C(7)–C(8) bonds. The five-membered ring of **4** is more puckered than in **2**: the sum of the absolute values of the internal torsion angles is 110.2(1)°. The *cis* amide bonds in either **2** or **4** are essentially planar, with the exception of that in the six-membered ring of **4** for which $\omega = -5.4(2)°$ was found.

The fusion between the two rings of compound **4** is of the *cis*-type as seen from the torsion angles of junction which are −40.3(2)° and −33.5(2)°, respectively, for the six- and five-membered ring, and both of the same sign. With respect to the six-membered ring of **4**, the axial character of H(8) is more pronounced than that of the H(9) atom. This can be appreciated considering the difference between the intra-ring torsion angles (Table 2) preceding and following the carbon atom bound to the hydrogen: the greater the difference, the more axial the character. The torsion angle of junction H(8)–C(8)–C(9)–H(9) is −36(2)°, and the contact distance H(8)···H(9) is 2.39(2) Å, slightly larger than in **2**. One of the axial hydrogen of the six-membered ring, that bound to C(7), is oriented on the same side of the five-membered ring, in contrast with compound **2** where all axial hydrogens are on the opposite side of the five-membered ring. The folding between the two rings of **4** can be described by the angle between the mean planes through the two rings' non-H atoms which is 123.3(1)° and larger than that of compound **2**.

Crystal Packing. The crystal packing of **2**, which is shown in Figure 3 on the *ac* plane, is characterized by two intermolecular hydrogen bonds, occurring between the NH and CO groups of screw-related molecules. Hydrogen-bonded molecules form infinite wavy ribbons elongating along the *a* direction: the packing of ribbons along the other two directions is governed mainly by van der Waals forces.

The crystal packing of **4**, which is shown in Figure 4 on the *ac* plane, is characterized by four intermolecular hydrogen bonds. The two amide groups are differently engaged in hydrogen-bonding interactions. The five-membered ring NH and CO groups of screw-related molecules form infinite hydrogen bonds along the *b* and *c* directions. Halfway along the *a* direction, the water molecules form hydrogen bonds with the NH and CO groups of the six-membered ring. In particular the water molecules are engaged in three hydrogen bonds, one as acceptor, with the six-membered ring NH group, the other two as donor, with the CO groups of the same ring.

***Ab Initio* Calculations.** As for the geometries of the two *cis* amide groups in the two bicyclic dilactams, relevant differences can be evidenced looking at the lengths of the N–C and C–O bonds. In contrast with compound **2**, where N–C and C–O bond lengths are comparable within the experimental errors, a shortening of the N–C bond and a lengthening of the C–O bond were observed in the piperidone ring of compound **4**, and not in the pyrrolidone ring. These experimental observations may indicate differences in the electronic structure of the two rigid dilactams (*i.e.*, the occurrence of a polar resonance form, $=N^+=C-O^-$, more evident in the six-membered ring of compound **4**), as well as geometrical differences due to the different crystal packing (Figures 3 and 4).

Since the degree of polarization of the amide group could be relevant in modulating the amnesia-reversal activity of 2-pyrrolidone-containing compounds,[16] the two hypotheses were evaluated by *ab initio* calculations. The geometries of the two isolated molecules, **2** and **4**, intermolecular complexes designed to mimic the crystal packings, namely the dimers of 2-piperidone, 2-pyrrolidone, and 2-piperidone solvated by three water molecules, were fully optimized with 3-21G, 6-31G, 6-31G*, and 6-31G** basis sets. The results are summarized in Table 3.

For both compounds **2** and **4**, the C–O double bond for the five-membered lactam moiety is shorter than the C–O double bond for the six-membered ring, likely due only to differences in ring size as confirmed by *ab initio* calculation results on 2-pyrrolidone- and 2-piperidone-isolated molecules. Since the results obtained with larger basis sets (6-31G* and 6-31G**) did not differ significantly from those obtained by smaller basis sets, the calculations on 2-pyrrolidone and 2-piperidone were performed using 3-21G and 6-31G basis sets only.

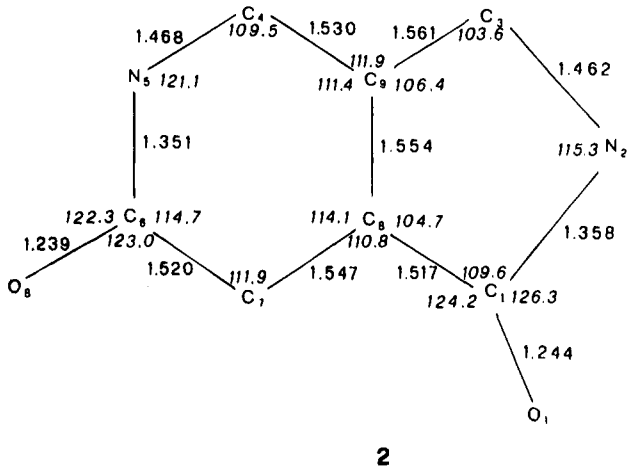

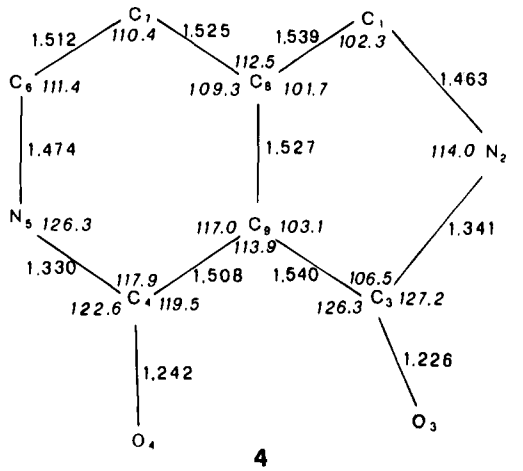

Figure 1. Atomic numbering schemes and valence bond lengths (Å) and angles (deg) for compounds **2** and **4**. ESDs are in the ranges of 0.003–0.004 Å and 0.2–0.3° (**2**) and 0.002–0.004 Å and 0.1–0.2° (**4**) for bond lengths and angles, respectively.

Table 1. Crystal Data for *cis*-Perhydropyrrolo[3,4-*c*]pyridine-1,6-dione (**2**) and *cis*-Perhydropyrrolo[3,4-*c*]pyridine-3,4-dione (**4**)

	compound	
	2	**4**
empirical formula	$C_7H_{10}N_2O_2$	$C_7H_{10}N_2O_2 \cdot H_2O$
formula weight	154.2	172.2
crystal system	monoclinic	monoclinic
a (Å)	11.918(8)	10.693(6)
b (Å)	6.453(14)	6.159(3)
c (Å)	9.609(12)	12.805(9)
β (deg)	95.51(8)	91.32(5)
V (Å^3)	736(2)	843.1(8)
space group	$P2_{1/c}$	$P2_{1/c}$
d_c (g cm^{-3})	1.39	1.36
Z	4	4
F(000)	328	368
λ(Mo Kα)	0.71069	0.71069
μ(Mo Kα) (mm^{-1})	0.11	0.12
crystal size (mm)	0.4 × 0.2 × 0.2	0.5 × 0.4 × 0.2
$2\theta_{max}$ (deg)	58	58
refl $I > 2.0\sigma(I)$	1405	1794
R, R_w	0.065, 0.092	0.055, 0.080
larg diff in ΔF synthesis (eÅ^{-3})	±0.25	±0.30
S	0.4	0.4
observation/parameter	14.1	16.5

Table 2. Relevant Torsion Angles (deg) for Compounds **2** and **4** (ESDs are in the range 0.2–0.3° for the torsion angles not involving H atoms)

	2	**4**
Five-Membered Ring		
C(1)–N(2)–C(3)–C(9)	5.0	−1.0
N(2)–C(3)–C(9)–C(8)	−5.7	22.4
C(3)–C(9)–C(8)–C(1)	4.7	−33.5
C(9)–C(8)–C(1)–N(2)	−1.8	32.7
C(8)–C(1)–N(2)–C(3)	−2.1	−20.6
Six-Membered Ring		
C(4)–N(5)–C(6)–C(7)	−3.2	24.6
N(5)–C(6)–C(7)–C(8)	−43.9	−50.7
C(6)–C(7)–C(8)–C(9)	40.8	58.7
C(7)–C(8)–C(9)–C(4)	5.6	−40.3
C(8)–C(9)–C(4)–N(5)	−49.7	13.7
C(9)–C(4)–N(5)–C(6)	52.0	−5.4
C(6)–C(7)–C(8)–C(1)	−77.0	170.8
N(5)–C(4)–C(9)–C(3)	69.3	−106.5
C(6)–C(7)–C(8)–H(8)	164.5	−67.2
N(5)–C(4)–C(9)–H(9)	−174.8	135.8
C(1)–C(8)–C(9)–C(4)	126.9	−159.3
C(7)–C(8)–C(9)–C(3)	−116.3	85.6
C(4)–C(9)–C(8)–H(8)	−119.0	79.6
C(7)–C(8)–C(9)–H(9)	124.6	−156.2
H(8)–C(8)–C(9)–H(9)	0.1	−36.4
N(2)–C(1)–C(8)–H(8)	−117.6	157.2
N(2)–C(3)–C(9)–H(9)	118.1	−97.5

The calculation results obtained on five- and six-membered lactams indicate large variations of the C–O double bond (and of the associated C–N single bond), the effect of solvation being larger than the effect of dimerization. These variations are in agreement with the difference observed on X-ray structures and led us to conclude that the elongation of the C–O bond in the six-membered ring of **4** depends mostly on crystal packing rather than on the occurrence of different polar forms.

Conformational Behavior. While compounds **2–5** are rigid, the absence of constraints due to ring fusion and the presence of the two ethoxycarbonyl groups are expected to induce large conformational flexibility in compounds **6** and **7**. Due to the relevance of molecular *rigidity/flexibility* in modulating physicochemical interactions underlying biological recognition processes, we investigated on the conformational behavior of the seven nootropics (**1–7**) by means of the high-temperature-quenched molecular dynamics (QMD) implemented in the molecular modeling software SYBYL.

QMD allows to rapidly generate the distribution of low-energy conformers with a large spread of structural properties.[22] It is known that, compared to other methods (*e.g.*, Monte Carlo techniques), QMD is poorer, not allowing a complete exploration of the conformational hyperspace.[23] Nevertheless, we choose QMD as a method for generating a meaningful ensemble of conformers, our goal being the exploration of the property variation within the maximum conformational space and not to locate minima. The results from QMD calculations are summarized in Table 4, where the total number of conformers generated and the number of conformers retained based on geometrical comparison (rms, see the Experimental Section), as well as relevant geometrical data (D_{O-O}), are reported.

With the exception of **6** and **7**, few conformers ($n = 5$ for piracetam; $n \leq 4$ for the others) were obtained. In contrast, 59 conformers were found for *cis*- (**6**) and 54 conformers for *trans*-4,5-bis(ethoxycarbonyl)-2-piperidone (**7**). These latter conformers were classified into three ring conformations (*i.e.*, two half-chairs, HC, and one twist-boat, TB). Conformers whose difference in the

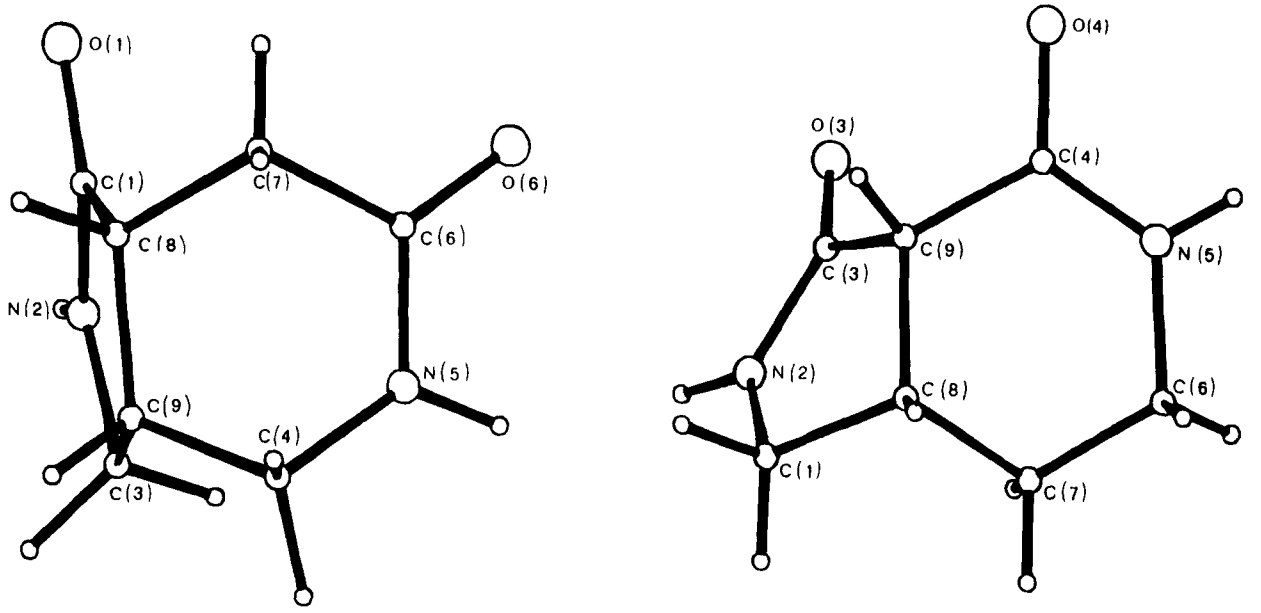

Figure 2. Perspective views of the crystal conformation of **2** and **4**.

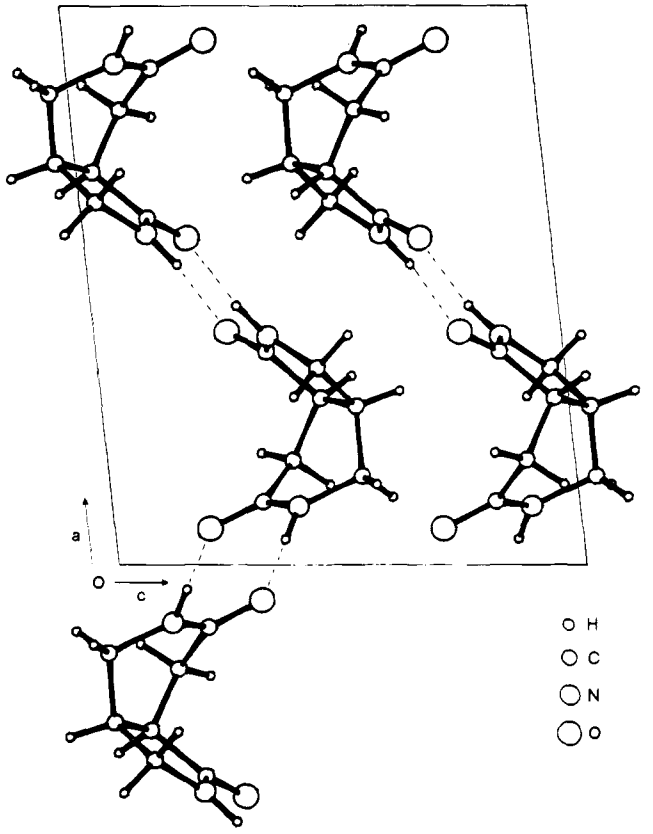

Figure 3. Crystal packing on the *ac* plane of **2**. Hydrogen bonds are shown by dashed lines.

dihedral angle H−C(4)−C(5)−H was within a tolerance of 30° were classified in the same ring conformation group. Due to the orientation of the ethoxycarbonyl groups, each ring conformation group included several conformational states with different stabilities.

The structure of the minimum-energy conformational state in each ring conformation was taken as representative of the class (Figure 5). The predicted structure and stability were in good agreement with those found in solution by NMR spectroscopy (see below).

NMR Spectroscopy. Information on the conformations of **2** and **4** in solution (D_2O and DMSO-d_6, respectively) were obtained from 1D and 2D ^{1}H-NMR spectra. ^{1}H decoupling, NOE differences, and COSY correlation maps confirmed the signal assignments from our preliminary NMR studies.[20] The Karplus equation[24] was used in determining dihedral angles between the protons at the junction (H(8)−C(8)−C(9)−H(9)).

While for compound **4** the coupling constant $J_{8,9}$ (8.1 Hz), easily measurable from the H(9) doublet at 3.00 ppm, indicated that the dihedral angle observed in the solid state (−36.4°) is essentially maintained in solution (*ca.* −35°), the signal patterns of H(8) and H(9) in compound **2** were more difficult to interpret, since they appeared as highly coupled spin systems. Irradiation of the H(3ax) at 3.56 ppm resulted in a loss of a 8.5-Hz coupling (corresponding to $J_{3ax,9}$) from the H(9) multiplet centered at 2.85 ppm, allowing to calculate a $J_{8,9}$ value of 9.8 Hz. The same value of $J_{8,9}$ could be calculated on the partially masked H(8) multiplet, irradiating alternatively H(7ax) at 2.57 ppm and H(7eq) at 2.40 ppm. Introduction of this value into the Karplus equation indicates an H(8)−C(8)−C(9)−H(9) angle of *ca.* 26°. Within the limits of the accuracy of prediction by the simplified Karplus equation used, this value is quite different from that observed in the solide state (0°) but close to that calculated on the low-energy conformations isolated by molecular dynamics (21−25°) and on *ab initio*-optimized geometries (3-21G, 36°; 6-31G, 23°; 6-31G*, 23°; 6-31G**, 25°). This finding may indicate that in solution the H(8) and H(9) atoms partially lose the character of totally eclipsed equatorial hydrogen atoms observed by X-ray diffraction analysis and, hence, that the conformational population of **2** in D_2O can not be described by the sole solid-state conformation.

As for the diester piperidones, the NMR spectra in $CDCl_3$[20] suggested a rapid equilibrium between ax−eq and eq−ax conformers (^{1}H-NMR: $J_{4,5}$ = 4.8 ± 0.8 Hz. ^{13}C-NMR: 170.3 ppm [CO(ester)]) for compound **6**, whereas for compound **7** they indicated that H(4) and H(5) are in a prevalent diaxial conformation (^{1}H-NMR: $J_{4,5}$ = 8.9 Hz. ^{13}C-NMR: 170.2 and 172.4 ppm [CO (ester)]). These results fully agree with the predictions made by QMD calculations. The energy values of the minimum-energy structures reported in Figure 5, in

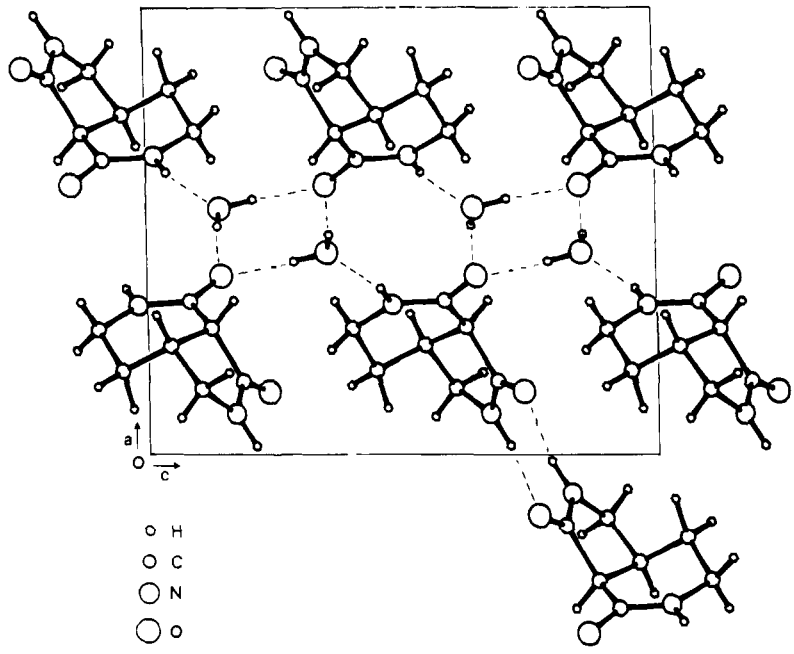

Figure 4. Crystal packing on the *ac* plane of **4**. Hydrogen bonds are shown by dashed lines.

Table 3. Comparison between Experimental (X-ray) and Calculated (*ab initio* methods, minimum-energy conformations) Bond Lengths for Amide Groups in Compounds **2**, **4**, 2-Pyrrolidone, and 2-Piperidone[a]

compounds	distances (Å)	X-ray	3-21G	6-31G	6-31G*	6-31G**
2	C(1)–O(1)	1.244	1.213	1.223	1.196	1.196
	C(1)–N(2)	1.358	1.357	1.352	1.352	1.352
	C(6)–O(6)	1.239	1.217	1.227	1.199	1.199
	C(6)–N(5)	1.351	1.357	1.356	1.356	1.356
4	C(3)–O(3)	1.226	1.208	1.217	1.191	1.191
	C(3)–N(2)	1.341	1.362	1.358	1.356	1.356
	C(4)–O(4)	1.242	1.215	1.225	1.195	1.196
	C(4)–N(5)	1.330	1.357	1.356	1.360	1.359
2-pyrrolidone						
isolated	C(1)–O(1)		1.213	1.224		
	C(1)–N(2)		1.361	1.355		
dimer	C(1)–O(1)		1.230	1.238		
	C(1)–N(2)		1.337	1.337		
	H bond		1.832	1.920		
2-piperidone						
isolated	C(1)–O(1)		1.221	1.231		
	C(1)–N(2)		1.356	1.355		
dimer	C(1)–O(1)		1.239	1.246		
	C(1)–N(2)		1.332	1.335		
	H bond		1.815	1.903		
solvated	C(1)–O(1)		1.257	1.258		
(three water	C(1)–N(2)		1.319	1.326		
molecules)	H bond 1		1.822	1.874		
	H bond 2		1.683	1.779		
	H bond 3		1.726	1.861		

[a] Detailed information on energy and geometry for all the compounds is available, upon request, from Swiss authors.

Table 4. Conformers Identified and Selected by QMD Calculations and Distance (Å) between Carbonyl Oxygens (D_{O-O}),[a] Taken as Representative of Interatomic Distances between Polar Groups, of the Piracetam-Type Nootropics Examined

compd	conf class[b]	no. of conformers[c] tot	sel	D_{O-O}^1	D_{O-O}^2	D_{O-O}^3	activity[d]
1		17	5	4.49	3.81	5.20	II
2		4	4	5.28	4.69	5.54	I
3		1	1	5.37	–	–	nt
4		4	4	2.99	2.99	3.32	III
5		1	1	2.99	–	–	III
6		145	59	3.76	3.64	5.91	III
	HCae		17	3.76	3.64	5.33	
	HCea		18	5.03	5.02	5.91	
	TB		24	5.01	3.79	5.78	
7		144	54	5.67	3.05	5.69	II
	HCee		12	3.76	3.76	5.37	
	HCaa		15	5.67	4.97	5.68	
	TB		27	5.03	3.05	5.69	

[a] For compounds **6** and **7**, D_{O-O} refers to the distance between carbonyl oxygen of lactam functionality (O(2)) and carbonyl oxygen of ethoxycarbonyl group in position 4. D_{O-O}^1 = O–O distance in the global minimum located by QMD; D_{O-O}^2 = lowest O–O distance identified by QMD; D_{O-O}^3 = highest O–O distance identified by QMD. D_{O-O} in the crystal structures of **2** and **4** were found to be 4.291 and 3.143 Å, respectively. [b] For compounds **6** and **7**, conformation classes are defined as follows: HC = half-chair; TB = twist-boat; ae = H(4ax)–H(5eq); ea = H(4eq)–H(5ax); ee = H(4eq)–H(5eq); aa = H(4ax)–H(5ax). [c] Total number (tot) of conformers identified by QMD and number of conformers selected (sel) with the criteria described in the Experimental Section (energy difference < 1.0 kcal/mol and relative rms < 0.33). [d] Criteria for establishing activity levels are described in the text. nt = not tested.

fact, indicated that, while for compound **6** ax–eq or eq–ax half-chair conformer families should be almost equally populated, a diaxial half-chair conformation should be preferred by compound **7**.

Partitioning Behavior. Lipophilicity of the cognition-activating agents examined here has been assessed by measuring octanol–water partition coefficients (log P_{oct}) and capacity factors (log k_w) in reversed-phase high-performance liquid chromatography (RP-HPLC). log P_{oct} values were determined by the classical "shake flask" method.[25] log k_w values (*i.e.*, capacity factors measured at 100% of aqueous mobile phase) were determined using two reversed phases, namely Deltabond C_8 (DB),[26] proposed to reduce effectively secondary adsorptive interactions, and an octadecylsilane (ODS) nonpolar stationary phase commonly used for lipophilicity measurements. The three lipophilicity data sets are reported in Table 5.

The lipophilicity rank order resulting from the RP-HPLC capacity factors (log k_w^{DB}, log k_w^{ODS}) is the same as that observed by log P_{oct} measurements, indicating that undesirable interactions with silanols and other

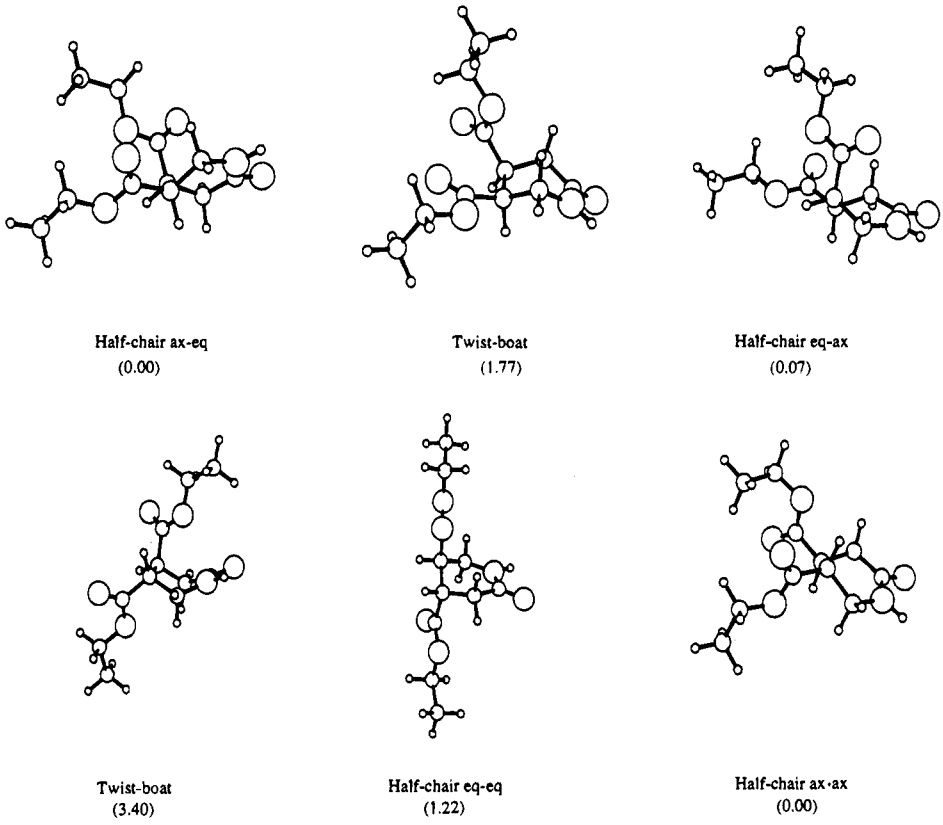

Figure 5. Ring conformations of *cis* and *trans* diester piperidones: minimum-energy structure for each class of conformers selected by QMD for compounds **6** (top) and **7** (bottom); the relative energy (kcal/mol) is given in parentheses.

Table 5. Lipophilicity Indices of the Investigated Lactam Derivatives

compd	log P_{oct}	log k_w^{DB}	log k_w^{ODS}	CLOG P	ΣMLP	ΣMLP$^+$	ΣMLP$^-$	log $P_{(MLP)}$[a]
1 (piracetam)	−1.54	−0.03	0.40	−1.49	−290.6	449.1	−739.7	−0.46
2	−2.11	−0.45	0.03	−2.80	−800.3	213.0	−1013.3	−1.73
3	−2.00	−0.36	0.20	−2.80	−804.5	213.4	−1017.9	−1.74
4	−1.95	−0.28	0.20	−1.88	−694.8	346.3	−1041.2	−1.40
5 (rolziracetam)	−1.11	0.43	0.97	0.46	−205.2	568.9	−774.1	−0.17
6	−0.03	1.28	1.83	0.84	132.7	946.9	−814.2	0.86
7	0.17	1.47	1.96	0.84	137.2	960.4	−823.2	0.88
2-pyrrolidone	−0.71	−0.13	0.37	−1.12	−83.3	424.6	−507.9	−0.04
2-piperidone	−0.47	0.20	0.75	−0.56	92.6	565.1	−472.5	0.45

[a] log $P_{(MLP)}$ represents the log P value predicted by using both negative and positive MLPs according to the equation reported in ref 27.

adsorptive sites did not significantly affect partitioning between the apolar stationary phases and the polar mobile phase. In order to unravel the structural information encoded in the lipopholicity parameters, a structure−lipophilicity relationship study was carried out.

Structure−Lipophilicity Relationships. The fragmental method of Hansch and Leo,[27] using the computer program CLOG P,[28] predicts quite well, at least in relative terms, the lipophilicity variations of the examined compounds. As expected, the method failed to predict the small but significant difference (0.1−0.2 log unit) between diastereoisomers **2/3** and **6/7** (*cis* more hydrophilic than *trans*).

In an attempt to model more accurately the lipophilicity variation in diastereoisomer pairs (**2/3**, **6/7**) and regioisomers (**2/4**), we calculated the molecular lipophilicity potential (MLP), using a method recently developed[29] and based on the atomic lipophilic fragmental system of Broto and Moreau.[30] MLPs were calculated by summation over the water-accessible surface area directly from the 3D-structure of the conformers selected by QMD.

Molecular Lipophilicity Potential. The MLPs, calculated as the MLP sum over the dots (ΣMLP), the MLP sum over all the dots with a MLP > 0 (ΣMLP$^+$), and the MLP sum over all the dots with a MLP < 0 (ΣMLP$^-$), are reported in Table 5. For each compound, ΣMLP, ΣMLP$^+$, and ΣMLP$^-$ are mean values calculated for all the conformers selected by QMD calculations.

A careful comparison of the lipophilicity parameters with MLP reveals that the difference in both log P and log k_w values between diastereomeric (**2/3**) and regioisomeric (**2/4**) bicyclic lactams mainly reflects the different accessibility of apolar moieties, accounted for by ΣMLP$^+$, rather than that of polar moieties, modeled by ΣMLP$^-$. Indeed, for isomers **2**−**4**, the increase of ΣMLP$^+$ is more significant than the decrease of ΣMLP$^-$. Thus, going from the 1,6-dione derivative (**2**) to the 3,4-dione isomer (**4**), it seems that the loss of hydrophilicity is due mainly to an increase of the apolar surface rather than to the proximity of polar groups as judged by CLOG P. Again, the increase of lipophilicity of the *trans*-1,6-dione derivative (**3**) with respect to the *cis* isomer (**2**) is predicted by ΣMLP$^+$. Similarly, the difference in lipophilicity between diastereomeric diester

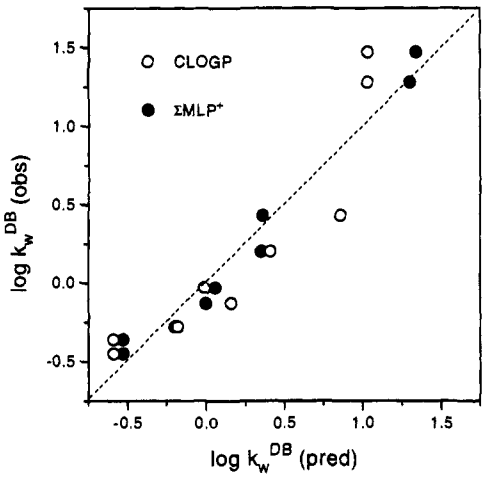

Figure 6. Plot of observed versus predicted log k_w^{DB}.

piperidones (**6**/**7**) seems due essentially to the ΣMLP^+, and the same quantitative order is conserved by ΣMLP.

Correlations of experimental parameters with MLP indicated ΣMLP^+ as the key parameter accounting for the lipophilicity variation within the whole set of lactam derivatives examined, as shown by eq 1, reported as an example:

$$\log k_w DB = 2.50 \times 10^{-3}(\pm 0.56 \times 10^{-3})\Sigma MLP^+ - 1.07(\pm 0.26) \quad (1)$$

$$n = 9 \quad r^2 = 0.972 \quad q^2 = 0.950 \quad s = 0.126 \quad F = 239.7$$

$$\log k_w DB = 0.45(\pm 022)\ \text{CLOG}\,P + 0.66(\pm 0.41) \quad (2)$$

$$n = 9 \quad r^2 = 0.835 \quad q^2 = 0.704 \quad s = 0.305 \quad F = 35.5$$

where n represents the number of data points, q^2 the squared cross-validated correlation coefficient, r^2 the squared correlation coefficient, s the standard deviation, and F the statistical significance of fit; the 95% confidence intervals are indicated in parentheses.

Figure 6 shows the plot of actual *versus* predicted log k_w^{DB} of the lactam derivatives and proves the potential of MLP approach in predicting lipophilicity parameters. In Table 6 the correlation matrix between experimental and computed indices of lipophilicity is reported. An examination of each single correlation revealed that the two simple lactams (2-pyrrolidone and 2-piperidone) are the strongest outliers. This points to peculiar solvation effects for compounds containing two or more polar groups relative to compounds containing only one polar group.

In summary the results reported here bring further evidence that the MLP approach, which takes into account conformational behavior and the dual information content of lipophilicity (*i.e.*, its hydrophobic part represented by the MLP summation over the surface and its polar part encoded in the fragmental atomic constants), can be more helpful than simple fragmental methods in interpreting and quantitatively predicting the partitioning behavior of molecules. In particular the ΣMLP^+ parameter is the best predictor for the lipophilicity behavior of the compounds studied. Due to opposite variations of ΣMLP^+ and ΣMLP, the prediction of lipophilicity of small diastereoisomers (**2**/**3**, **6**/**7**) is not clearly achieved when the summation of MLP (ΣMLP) is used. Generally, MLP is more sensitive to large variations of accessible surface area (ASA), *i.e.*, conformation of large molecules or relevant variations between topological isomers, than to more limited differences of ASA such as those existing between small diastereoisomers.[31] Further work is required to improve accuracy and sensitivity of the MLP approach in the prediction of lipophilicity.

Insights into Structure–Activity Relationships. Qualitative relations have been examined between lipophilicity and polarity properties, on the one hand, and *in vivo* activity of the piracetam-type nootropics on the other hand. Although the mechanism of action of these drugs is poorly understood, the search for new drugs in this area generally relies on behavioral tests.[32,33] In particular the reversal of the experimentally induced (by scopolamine,[34] ECS,[35] or hypoxia[36]) amnesia in a passive avoidance test has been widely used for screening purposes.[14,15,35,37-39] On the basis of the amnesia-reversal activity data,[20] we could rank the piracetam analogs under investigation into three groups: *i.e.*, strongly (III), moderately (II), and weakly active (I).

Compounds **4** and **6** being more potent than piracetam (**1**) belong to group III, whereas dilactam **2** (less active than piracetam) is classified into group **I**. *trans*-Dicarbethoxypiperidone (**7**) and piracetam are of moderate potency (group II).

Within the limits of the examined physicochemical space, it can be observed that lipophilicity does not influence the *in vivo* activity, whereas the properties of the polar groups, especially the H-bonding properties of carbonyl oxygens, seem to be more relevant for the pharmacological properties. Recently, Cosentino *et al.*[19] identified a common spatial disposition of the polar functional groups present in a series of piracetam-type nootropics and suggested two possible pharmacophoric models (Figure 7). Using conformational analysis and chemometric methods, these authors identifyied three interatomic distances (D_{O-O}, D_{C-C}, and D_{N-X}) as the most relevant ones in defining the topology of the polar groups present in the 2-pyrrolidone-containing nootropics (an N–C=O amidic group and a X–C=O group, with X = O, N).

Our results confirm that D_{O-O} has to be below 4 Å, in agreement with the proposed pharmacophores, and furthermore suggest that an inverse relation should exist between the antiamnesic properties and the distance separating the carbonyl oxygens (D_{O-O}). Table 4 reports the D_{O-O} distance calculated for the conformers selected by our QMD calculations. Dilactam **4** (D_{O-O} *ca.* 3 Å) is more active than piracetam (**1**) (D_{O-O} *ca* 4.5 Å), whereas compound **2** (D_{O-O} > 5 Å) is the least active. Compound **5** (rolziracetam),[37] whose D_{O-O} is very close to 3 Å, is a good cognition enhancer (group III). As for the dicarbethoxypiperidones (**6**, **7**), the *cis* diastereoisomer (**6**, group III) can adopt relatively low-energy conformations whose D_{O-O} are between 4 and 5 Å (global minimum: D_{O-O} = 3.76 Å), whereas the *trans* diastereoisomer (**7**), belonging to group II, should prefer conformations whose geometries should be very close to that of the global minimum (D_{O-O} = 5.67 Å), as

Table 6. Squared Correlation Matrix[a] between Lipophilicity Indices

	log P_{oct}	log k_w^{DB}	log k_w^{ODS}	CLOG P	ΣMLP	ΣMLP$^+$	ΣMLP$^-$
log k_w^{DB}	0.775 (0.998)						
log k_w^{ODS}	0.781 (0.993)	0.996 (0.997)					
CLOG P	0.792 (0.858)	0.835 (0.871)	0.839 (0.870)				
ΣMLP	0.923 (0.922)	0.631 (0.912)	0.630 (0.893)	0.785 (0.908)			
ΣMLP$^+$	0.846 (0.985)	0.972 (0.983)	0.964 (0.972)	0.880 (0.887)	0.746 (0.943)		
ΣMLP$^-$	0.355 (0.403)	0.038 (0.384)	0.039 (0.362)	0.186 (0.539)	0.554 (0.661)	0.094 (0.423)	
log $P_{(MLP)}$	0.950 (0.947)	0.734 (0.939)	0.733 (0.922)	0.846 (0.913)	0.987 (0.997)	0.838 (0.966)	0.440 (0.606)

[a] Squared correlation coefficients calculated excluding 2-pyrrolidone and 2-piperidone from regression analysis are reported in parentheses.

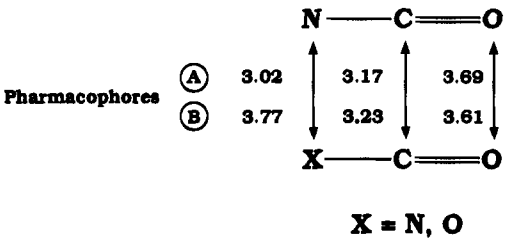

Figure 7. Possible pharmacophores proposed for 2-pyrrolidone-containing nootropics (see ref 19). The distances are expressed in Å.

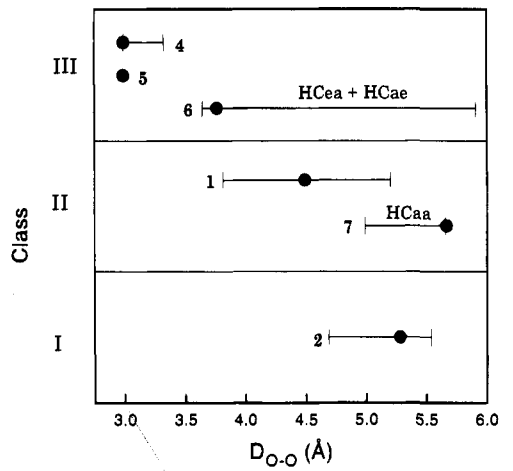

Figure 8. Plot of the amnesia-reversal activity (levels I, II, and III as defined in the text) versus the distance (Å) between the carbonyl oxygens (D_{O-O}), taken as representative of distances between polar groups (see Table 4). The filled circles represent D_{O-O} in the global minimum-energy conformations. The bars span the higher energy conformers also selected by QMD. For compounds **6** and **7**, only conformers compatible with NMR data have been represented (see discussion in the text).

demonstrated by NMR data and QMD results. A graphical representation of this relationship is reported in Figure 8.

It was noted[19] that the only significant difference in the two pharmacophore models proposed (Figure 7) is the D_{N-X} distance and that activity data for rigid compounds should allow the selection between them. Looking at our rigid dilactams (**2**, D_{N-N} = 4.25 Å; **4**, D_{N-N} = 4.10 Å), pharmacophore B may be more realistic than pharmacophore A. However, due to the limited number of compounds examined, no firm conclusion can be reached at this stage.

Conclusions

Analysis of crystallographic data for rigid bicyclic dilactams **2** and **4** provided indications about differences between the geometries of the *cis* amide groups. *Ab initio* calculations on intermolecular complexes of **2** and **4** reproduced these differences demonstrating their dependence on crystal packing rather than on electronic properties of the isolated molecules.

Lipophilicity does not play a relevant role in determining the activity of the examined series, most likely because the examined compounds are too small and highly functionalized, whereas the importance of the distance between carbonyl oxygens in influencing the amnesia-reversal activity of piracetam-type compounds is indicated by the conformational properties of lactam analogs. The results obtained by high-temperature QMD calculations were in good agreement with NMR data.

Together with the findings of other investigations on the structure and conformation of nootropics,[16-19] our results, based on the selection of the pharmacophoric distances from the entire conformational range, can be of significance in the design of new piracetam-like cognition enhancers. While compounds **4** and **6** are among the most active lactam-containing nootropics[40] designed and synthesized by us to date, much progress can be expected from the modern tools of drug design.

Experimental Section

Chemicals. Lactam derivatives **2**–**4**, **6**, and **7** were synthesized as already reported.[20] A pure sample of dihydro-1*H*-pyrrolizine-3,5(2*H*,6*H*)-dione ('rolziracetam') was kindly provided by Parke Davis/Warner-Lambert Co. (Ann Arbor, MI). Piracetam was purchased from Sigma Chemical Co. (St. Louis, MO). Other chemicals were purchased from Aldrich Chemical Co. (Milwaukee, WI).

Crystal Structure Determination. Single crystals of **2** and **4** were obtained from methanol and ethanol solutions, respectively, by slow evaporation. Approximate unit-cell parameters and the space group of both compounds were determined by oscillation and Weissenberg photographs. A four-circle SINTEX $P2_1$ diffractometer equipped with Mo Kα radiation and graphite monochromator was used for intensity data collection of both compounds. The refined unit-cell parameters, determined by a least-squares fit of the angular setting of 14 reflections in the range $10° < \theta < 20°$ for **2** and and 16 reflections in the range $10° < \theta < 25°$ for **4**, are given in Table 1. A total of 2377 and 2613 independent reflections were collected respectively for compounds **2** and **4** by the $\theta - 2\theta$ technique with a scan speed within the interval 1.5–29.3°

min^{-1} over a range of 1.6°. Background counts were taken for a time equal to half the scan time. X-ray decay was taken into account by three standard reflections, monitored after every 100 collected reflections. A least-squares fit of intensity of each standard reflection versus data collection number showed an overall linear decay rate in both compounds. An overall intensity variation of about 5% and 7% was noted for compounds **2** and **4**, respectively, and a corresponding decay factor was calculated and applied to each reflection. Lorentz and polarization but no absorption corrections were applied.

Both structures were solved by direct methods using the program MULTAN 80.[41] Isotropic and anisotropic refinement of the non-H atoms were carried out by the full-matrix least-squares method minimizing the function $\Sigma w(|F_o| - |F_c|)^2$ where $w = (a + |F_o| + c|F_o|^2)^{-1}$ with a and c equal to $2F_{o(min)}$ and $2F_{o(max)}$, respectively. The final difference Fourier synthesis revealed all the H atoms for both compounds. The H atoms were introduced in the last structure calculation with isotropic thermal values deduced from the carrier atoms. Scattering factors were taken from ref 42. Observed and calculated structure factors and anisotropic thermal parameters of the non-H atoms have been deposited. All the calculations were carried out on the D.G. ECLIPSE MV/8000 II using the package of programs of ref 43.

Lipophilicity Measurements. Partition coefficients were determined in 1-octanol and pH 7.4 phosphate buffer (0.05 M) at room temperature. Drug concentrations in aqueous phase before partitioning were within the range 1×10^{-4}–1×10^{-3} M. At equilibrium, concentrations were measured in the aqueous phase by HPLC after centrifugation.

As further lipophilicity parameters, the capacity factors at 100% water eluent (log k_w) were determined as already described.[26] The mobile phase consisted of 0.05 M acetate buffer (pH 5.0). A 5-μm Deltabond C_8 column (159 × 3.9 mm i.d.; Keystone Sci., Belfonte, PA) or a 10-μm μ-Bondapak C_{18} column (150 × 3.9 mm i.d.; Waters Assoc., Milford, MA) were used as stationary phases. All chromatographic measurements were performed at a constant temperature of 30 ± 0.5 °C and a flow rate of 1 mL/min on a Waters HPLC Model 600 multisolvent delivery system (Waters Assoc., Milford, MA) equipped with a Waters 481 variable wavelength detector operating at 210 nm. Calculated log P_{oct} values were obtained by the fragmental method of Hansch and Leo[27] using the CLOG P 3.54 software.[28]

NMR Spectroscopy. ^{1}H-NMR spectra were recorded at 25 °C for solutions of compounds **2** and **4** in D_2O and DMSO-d_6, respectively, at 300 MHz on a Bruker AM300WB spectrometer. The signal position was recorded with reference to the external standard TMS.

***Ab Initio* Calculations.** The *ab initio* calculations were performed on a Silicon Graphics Indigo workstation with the Gaussian 90 software and on the Cray 2 supercomputer of the Ecole Polytechnique Fédérale de Lausanne with the Gaussian 92 software.[44] In both cases, the geometry optimization was performed with the Berny algorithm using the default convergence criteria; the direct method was used to solve the SCF equations.

Molecular Dynamics Calculations. All the calculations were performed using the SYBYl 5.5 and 6.0 softwares[45] on Silicon Graphics Personal Iris 4D/35, Power Series 4D/320, or Indigo R4000 workstations. The geometry optimizations were performed with the Tripos force field[46] including an electrostatic term calculated with Gasteiger–Marsili partial atomic charges[47] and a dielectric constant $\epsilon = 1$. The Powell algorithm was used for the geometry optimization with a convergence obtained when the gradient was lower than 0.001 kcal/mol Å^2. The dynamics simulations were performed in absence of water in a completely automated mode monitored with SPL macrocommands. The comparison of molecules was performed with the SYBYL MATCH option using all heavy atoms and all polar hydrogens. The absolute rms was recorded for each pairwise comparison and the highest rms over all the comparisons determined. This allows to derive a relative rms for each comparison. The dynamics strategy used in this study was the following: (1) For each compound a starting geometry was fully optimized, in order to eliminate unfavorable steric interactions, and a dynamics simulation at 2000 K during 100 ps was performed. Starting with a Boltzmann distribution of the atomic velocities, the Newton second equation was solved each 1 fs, and 2000 different geometries were selected along the trajectory. (2) From the retained geometries, only 200 conformers were randomly selected. Their geometries were completely optimized, and all the conformers were classified by increasing energy. (3) The comparison for each pair of conformers was performed and their relative rms determined. Two arbitrary criteria were used to judge the similarity between two different conformers: their energy difference must be lower than 1 kcal/mol and their relative rms must be lower than 33%. In the case of identical geometries, the highest energy conformer was eliminated from the database.

Molecular Lipophilicity Potential. The molecular lipophilicity potential (MLP) used in our application[29] is based on the slightly modified Fauchère equation[48] and the atomic lipophilic fragmental system of Broto and Moreau.[30] Starting with two files generated by SYBYL, *i.e.*, one containing the molecule geometry (mol2 file format) and a second containing the coordinates of points onto the accessible surface (dot file format), a FORTRAN program was written to identify automatically the atomic fragments, then to calculate the potential at each dot onto the water-accessible surface area, and then to generate new parameters (ΣMLP, ΣMLP$^+$, and ΣMLP$^-$).

Acknowledgment. The authors wish to thank Mr. Trabassi for providing drawings and Parke Davis/Warner-Lambert Co. (Ann Arbor, MI) for the kind gift of a pure sample of 'rolziracetam'. The Italian authors are indebted to MURST and CNR, whereas the Swiss authors are indebted to the Swiss National Science Foundation for financial support.

Supplementary Material Available: X-ray data including final fractional coordinates, thermal parameters (Å^2), and relevant geometrical details of the intermolecular hydrogen bonds of **2** and **4** and molecular modeling results including relative energy, MLP parameters, and D_{O-O}, taken as representative of interatomic distances between polar groups, for conformations of piracetam-type nootropics selected by QMD calculations (9 pages); tables of observed and calculated structure factors for **2** and **4** (21 pages). Ordering information is given on any current measthead page.

References

(1) Hershenson, F. M.; Moos, W. H. Drug development for senile cognitive decline. *J. Med. Chem.* **1986**, *29*, 1125–1130.
(2) Kan, J. P. Current and future approaches to therapy of Alzheimer's disease. *Eur. J. Med. Chem.* **1992**, *27*, 565–570 and references cited therein.
(3) FDA committee endorses Warner-Lambert's tacrine. *Scrip* **1993**, March *26*, 19.
(4) Fröstl, W.; Maitre, L. The families of cognition enhancers. *Pharmacopsychiatry* **1989**, *22*, 54–100.
(5) Dolmella, A.; Bandoli, G.; Nicolini, M. Alzheimer's disease: a pharmacological challenge. In *Advances in Drug Research*; Testa, B., Meyer, U. A., Eds.; Academic Press, Inc.: San Diego, 1994; Vol. 25, pp 203–294.
(6) Gamzu, E. R.; Hoover, T. M.; Gracon, S. I.; Ninteman, M. V. Recent developments in 2-pyrrolidone-containing nootropics. *Drug Dev. Res.* **1989**, *18*, 177–189.
(7) Viana, G. S. B.; Marinho, M. M. F.; Sousa, F. C. F. Effect of piracetam administration of ^3H-N-methylscopolamine binding in cerebral cortex of young and old rats. *Life Sci.* **1992**, *50*, 971–977.
(8) Maillis, A.; Karayanidis, F.; Koutsoukos, E.; Angelipoulos, E.; Stefanis, C. Effect of piracetam on single central neurons. *Neuropsychobiology* **1988**, *19*, 139–145.
(9) Beukers, M.; Boddeke, E. W. G. M. Pharmacology of long-term potentiation. A model for learning reviewed. *Pharm. Weekbl., Sci. Ed.* **1991**, *13*, 7–12.
(10) Satoh, M.; Ishihara, K.; Iwama, T.; Takagi, H. Aniracetam augments, and midazolam inhibits, the long-term potentiation in guinea pig hippocampal slices. *Neurosci. Lett.* **1986**, *68*, 216–220.
(11) Marchi, M.; Besana, E.; Raiteri, M. Oxiracetam increases the release of endogenous glutamate from depolarized hippocampal slices. *Eur. J. Pharmacol.* **1990**, *185*, 247–249.

(12) Pugliese, A. M.; Corradetti, R.; Ballerini, L.; Pepeu, G. Effect of nootropic drug oxiracetam on field potential of rat hippocampal slices. *Br. J. Pharmacol.* **1990**, *99*, 189–193.
(13) Rosemberg, D. R.; Wright, B. A.; Gershon, S. Cognitive enhancing agents for the treatment of senile dementia of the Alzheimer's type. *Drugs. Today* **1990**, *26*, 449–471.
(14) Pinza, M.; Farina, C.; Cerri, A.; Pfeiffer, U.; Riccaboni, M. T.; Banfi, S.; Biagetti, R.; Pozzi, O.; Magnani, M.; Dorigotti, L. Synthesis and pharmacological activity of a series of dihydro-1*H*-pyrrolo[1,2-a]imidazole-2,5(3*H*,6*H*)-diones, a novel class of potent cognition enhancers. *J. Med. Chem.* **1993**, *36*, 4214–4220.
(15) Angelucci, L.; Calvisi, P.; Catini, R.; Cosentino, U.; Cozzolino, R.; De Witt, P.; Ghirardi, O.; Giannessi, F.; Giuliani, A.; Guaraldi, D.; Misiti, D.; Ramacci, M. T.; Scolastico, C.; Tinti, M. O. Synthesis and amnesia-reversal activity of a series of 7- and 5-membered 3-acylamino lactams. *J. Med. Chem.* **1993**, *36*, 1511–1519.
(16) Bandoli, G.; Grassi, A.; Liégeois, C.; Lumbroso, H.; Montoneri, E.; Pappalardo, G. C. X-ray crystal structure, dipole moment and theoretical molecular orbital study of the cognition activator dihydro-1*H*-pyrrolizine-3,5(2*H*,6*H*)-dione ('rolziracetam'). *Eur. J. Med. Chem.* **1989**, *24*, 81–85.
(17) Amato, M. E.; Bandoli, G.; Grassi, A.; Marletta, A.; Perly, B. X-ray, NMR and theoretical studies of the structure and conformation of the nootropic agent Tenilsetam. *Eur. J. Med. Chem.* **1991**, *26*, 443–448.
(18) Cosentino, U.; Scolastico, C.; Moro, G.; Morosi, G.; Pitea, D. The influence of the calculation method on conformational analysis of pyrrolidin-2-one derivatives. *Mol. Struct., THEOCHEM* **1989**, 199–212.
(19) Cosentino, U.; Moro, G.; Pitea, D.; Todeschini, R.; Brossa, S.; Gualandi, F.; Scolastico, C.; Giannessi, F. Pharmacophore identification in amnesia-reversal compounds using conformational analysis and chemometric methods. *Quant. Struct.–Act. Relat.* **1990**, *9*, 195–201.
(20) Altomare, C.; Carotti, A.; Casini, G.; Cellamare, S.; Ferappi, M.; Gavuzzo, E.; Mazza, F.; Pantaleoni, G.; Giorgi, R. Synthesis and cognition activating properties of some mono- and bicyclic lactam derivatives. *J. Med. Chem.* **1988**, *31*, 2153–2158.
(21) Klyne, W.; Prelog, V. Description of steric relationships across single bonds. *Experientia* **1960**, *16*, 521–528.
(22) O'Connor, S. D.; Smith, P. E.; Al-Obeidi, F.; Pettitt, B. M. Quenched Molecular Dynamics Simulations of Tuftsin and Proposed Cyclic Analogues. *J. Med. Chem.* **1992**, *35*, 2870–2881.
(23) (a) Ghose, A. K.; Jaeger, E. P.; Kowalczyck, P. J.; Peterson, M. L.; Treasurywala, A. M. Conformational Searching Methods for Small Molecules. I. Study of the SYBYL SEARCH Method. *J. Comput. Chem.* **1993**, *14*, 1050–1065. (b) Judson, R. S.; Jaeger, E. P.; Treasurywala, A. M.; Peterson, M. L. Conformational Searching Method for Small Molecules. II. Genetic Algorithm Approach. *J. Comput. Chem.* **1993**, *14*, 1407–1414. (c) Morley, S. D.; Jackson, D. E.; Saunders, M. R.; Vinter, J. G. DMC: A Multifunctional Hybrid Dynamics/Monte Carlo Simulation Algorithm for the Evaluation of Conformational Space. *J. Comput. Chem.* **1992**, *13*, 693–703.
(24) Jackman, L. M.; Sternhell, S. *Application in Organic Chemistry*, 2nd ed.; Pergamon Press: London, 1969.
(25) Leo, A.; Hansch, C.; Elkins, D. Partition coefficients and their use. *Chem. Rev.* **1971**, *71*, 525–616.
(26) Altomare, C.; Cellamare, S.; Carotti, A.; Ferappi, M. Linear Solvation Energy Relationships in reversed-phase liquid chromatography. Examination of Deltabond C_8 as stationary phase for measuring lipophilicity parameters. *Quant. Struct.-Act. Relat.* **1993**, *12*, 261–268.
(27) Hansch, C.; Leo, A. The FRAGMENT method of calculating partition coefficients. *Substituents constants for correlation analysis in chemistry and biology*; Wiley-Interscience: New York, 1979; pp 18–43.
(28) Pomona College Medicinal Chemistry Project, Claremont, CA.
(29) (a) Gaillard, P; Carrupt, P. A.; Testa, B.; Boudon, A. Molecular Lipophilicity Potential, a tool in 3D QSAR. Method and applications. *J. Comput.-Aided Mol. Des.* **1994**, *8*, 83–96. (b) Gaillard, P.; Carrupt, P. A.; Testa, B. The conformation-dependent lipophilicity of morphine glucuronides as calculated from their Molecular Lipophilicity Potential. *Bioorg. Med. Chem. Lett.* **1994**, *4*, 737–742.
(30) Broto, P.; Moreau, G.; Vandycke, C. Molecular structures: Perception, autocorrelation descriptor and SAR studies. *Eur. J. Med. Chem.* **1984**, *19*, 71–78.
(31) Tsai, R. S.; Carrupt, P. A.; Testa, B.; El Tayar, N.; Grunewald, G. L.; Casy, A. F. Influence of stereochemical factors on the partition coefficient of diastereoisomers in a biphasic octan-1-ol/water system. *J. Chem. Res.* **1993**, (S) 298–299, (M) 1901–1920.
(32) Schindler, U. Pre-clinical evaluation of cognition enhancing drugs. *Prog. Neuro-Psychopharmacol. Biol. Psychiatry* **1989**, *13* (Suppl.), 99–115.
(33) (a) Sarter, M.; Hagan, J.; Dudchenko, P. Behavioral screening for cognition enhancers: from indiscriminate to valid testing: Part 1. *Psychopharmacology* **1992**, *107*, 144–159. (b) Sarter, M.; Hagan, J.; Dudchenko, P. Behavioral screening for cognition enhancers: from indiscriminate to valid testing: Part 2. *Psychopharmacology* **1992**, *107*, 461–473.
(34) Schindler, U.; Rush, D. K.; Fielding, S. Nootropic drugs: animal models for studying effects on cognition. *Drug Dev. Res.* **1984**, *4*, 567–576.
(35) Butler, D. E.; Nordin, I. C.; L'Italien, Y. J.; Zweisler, L.; Poschel, P. H.; Marriott, J. G. Amnesia-reversal activity of a series of N-[(disubstituted-amino) alkyl]-2-oxo-1-pyrrolidineacetamides, including Pramiracetam. *J. Med. Chem.* **1984**, *27*, 684–691.
(36) Giurgea, C.; Salama, M. Nootropic Drugs. *Prog. Neuro-Psychopharmacol.* **1977**, *1*, 235–247.
(37) Butler, D. E.; Leonard, J. D.; Caprathe, B. W.; L'Italien, Y. J.; Pavia, M. R.; Hershenson, F. M.; Poschel, P. H.; Marriott, J. G. Amnesia-reversal activity of a series of cyclic imides. *J. Med. Chem.* **1987**, *30*, 498–503.
(38) Toja, E.; Gorini, C.; Zirotti, C.; Barzaghi, F.; Galliani, G. Amnesia-reversal activity of a series of 5-alkoxy-1-arylsulfonyl-2-pyrrolidinones. *Eur. J. Med. Chem.* **1991**, *26*, 403–413.
(39) Levin, J. I.; Epstein, J. W.; Beer, B.; Dean, W. D.; Dusza, J. P.; Tseng, S.-S.; Schweitzer, H. J.; Francisco, G. D.; Cain, W. T.; Bartus, R. T.; Dean, R. L., III. Synthesis of substituted 5-amino-8-phenyl-3*H*,6*H*-1,4,5a,8a-Tetraazaacenaphtalen-3-ones, a new class of agents for the improvement of cognition. *Bioorg. Med. Chem. Lett.* **1991**, *1*, 435–440.
(40) Casini, G.; Ferappi, M. It. Pat. n. 1205709, March 31, 1989.
(41) Main, P.; Fiske, S. J.; Hull, S. E.; Lessinger, L.; Germain, G.; Declercq, J. P.; Woolfson, M. M. A System of Computer Programs for the Automatic Solution of Crystal Structures from X-ray Diffraction Data. MULTAN 80, 1990, Univ. of York, England, and Louvain, Belgium.
(42) *International Tables for X-ray Crystallography*; Kynoch Press: Birmingham, 1974; Vol. IV.
(43) Camalli, M.; Capitani, D.; Cascarano, G.; Cerrini, S.; Giacovazzo, C.; Spagna, R. SIR-CAOS (It. pat. n. 35403c/86): User Guide, 1986, Istituto di Strutturistica Chimica CNR, C.P. n° 10, 00016 Monterotondo Stazione, Roma, Italy.
(44) Frish, M. J.; Trucks, G. W.; Head-Gordon, M.; Gill, P. M. W.; Wong, M. W.; Foresman, J. B.; Johnson, B. G.; Schlegel, H. B.; Robb, M. A.; Replogle, E. S.; Gomperts, R.; Andres, J. L.; Raghavachari, K.; Binkley, J. S.; Gonzalez, C.; Martin, R. L.; Fox, D. J.; DeFrees, D. J.; Baker, J.; Stewart, J. J. P.; Pople, J. A. GAUSSIAN 92 software; Gaussian, Inc.: Pittsburgh, PA, 1992.
(45) SYBYL: Molecular Modelling Software, Tripos Assoc., St. Louis, MO.
(46) Clark, M.; Cramer, R. D., III; Van Opdenbosch, N. Validation of the general purpose Tripos 5.2 force field. *J. Comput. Chem.* **1989**, *10*, 982–1012.
(47) Gasteiger, J.; Marsili, M. Iterative partial equalization of orbital electronegativity: a rapid access to atomic charges. *Tetrahedron* **1980**, *36*, 3219–3222.
(48) Fauchère, J. L.; Quarendon, P.; Kaetterer, L. Estimating and representing hydrophobicity potential. *J. Mol. Graph.* **1988**, *6*, 202–206.

JM940241F